Desalination and Water Treatment
www.deswater.com

doi: 10.5004/dwt.2019.24424

159 (2019) 121–129
August

A novel Fe-containing clinoptilolite for wastewater remediation: degradation of azo-dyes acid orange 7 by H_2O_2 and ascorbic acid

M. Dosa[a], M. Piumetti[a,*], C. Galletti[a], N. Russo[a], D. Fino[a], S. Bensaid[a], G. Mancini[b], F.S. Freyria[a], G. Saracco[a]

[a]*Department of Applied Science and Technology, Politecnico di Torino, Turin, Italy, emails: marco.piumetti@polito.it (M. Piumetti), melodj.dosa@polito.it (M. Dosa), camilla.galletti@polito.it (C. Galletti), nunzio.russo@polito.it (N. Russo), debora.fino@polito.it (D. Fino), samir.bensaid@polito.it (S. Bensaid), francesca.freyria@polito.it (F.S. Freyria), guido.saracco@polito.it (G. Saracco)*
[b]*Department of Industrial-Mechanical Engineering, University of Catania, Catania, Italy, email: giuseppe.mancini@unict.it*

Received 15 November 2018; Accepted 17 May 2019

ABSTRACT

A novel 3 wt.% Fe-containing clinoptilolite catalyst was prepared starting from a natural zeolite followed by a ion-exchange synthesis. A Fe-containing ZSM-5 catalyst (commercial zeolite as support) was also prepared for comparison purpose. Both Fe-based catalysts, along with the unexchanged samples, were characterized by complementary techniques (e.g. X-ray powder diffraction (XRD), N_2 physisorption at –196°C, transmission electron microscopy (TEM), field emission scanning electron microscopy (FESEM), energy dispersive X-ray spectrometry (EDS) microanalysis). Then, their possible application in wastewater remediation was tested with a solution of azo-dyes acid orange 7 (AO7), as target molecule for azo dyes. As a whole, remarkable results in the AO7 degradation were obtained with the Fe-clinoptilolite in the presence of both ascorbic acid (AA) and H_2O_2. Specifically, AO7 conversion of about 60% was observed over the Fe-clinoptilolite (reaction time = 60 min). Lower performances were achieved in the presence of Fe-ZSM-5 coupled with ascorbic acid and H_2O_2 (AO7 conversion ~ 40%, t = 60 min.), despite the significantly higher SSA of the commercial ZSM-5. Noteworthy, the beneficial role of the ascorbic acid coupled with H_2O_2 was observed for both Fe-containing catalysts, thus confirming the key role of both oxidant and reductant agents in Fenton-like processes.

Keywords: Natural zeolites; Azo-dyes; Fenton chemistry; Wastewater remediation

1. Introduction

Over the years, the interest toward the clinoptilolite, one of the most useful naturally occurring zeolites, significantly increased due to its possible applications in various areas such as industry, agriculture, environmental protection, and even medicine [1–3]. In particular, clinoptilolite is probably the most used natural zeolite for the adsorption of either organic molecules or metal ions in the wastewater treatment [4–9]. Suitability for these applications is related to its good textural and structural properties, high resistance to extreme temperatures and chemically neutral basic structure. Moreover, the clinoptilolite framework $(Na_4 K_4)(Al_8 Si_{40}O_{96})$ $24H_2O$ contains cavities in the form of channels and cages (3.9 × 5.4 Å) occupied by H_2O molecules and extra-framework cations (K^+, Na^+, Ca^{2+} and Mg^{2+}) that are commonly exchangeable. However, an efficient ion exchange between the starting zeolite in aqueous solution and the salt, which contains the desired in-going cation, allows obtaining the desired metal-containing zeolite. In this scenario, Fe-containing zeolites seem to be an

* Corresponding author.

Presented at the 6th International Conference on Sustainable Solid Waste Management (NAXOS 2018), 13-16 June 2018, Naxos Island, Greece.

effective system for Fenton-type mechanism in water remediation. Fe-doped materials generally follow a Fenton-like mechanism, which is known to occur not only in solution, but also with heterogeneous catalysts, where both surface Fe^{2+} and Fe^{3+} ions react with H_2O_2 to form hydroxyl radicals [10–12].

Moreover, our recent works on the degradation of the azo-dyes acid orange 7 (AO7) over Fe-TiO_2 systems [10–12] have confirmed that the Fenton-type mechanism can be promoted in the presence of both hydrogen peroxide and ascorbic acid (Fenton-like agents) in solution.

In the present study, a novel 3 wt.% Fe-containing clinoptilolite sample was prepared by cation-exchange method. Similarly, a Fe-containing ZSM-5 sample was prepared for comparison. The idea is to compare natural clinoptilolite to a commercial ZSM-5 to see which product has the better performance toward AO7 degradation. The prepared catalysts were characterized by physico-chemical techniques (XRD, N_2 physisorption at –196°C, TEM, FESEM and EDS analysis). Catalysts activity was tested in dark conditions for the degradation of AO7 in aqueous solution, a rather stable azo-dyes pollutant, in the presence of either H_2O_2 or ascorbic acid as oxidant/reductant agents, respectively.

2. Materials and methods

2.1. Materials preparation

Both the 3 wt.% Fe-Clinoptilolite (herein labelled as Fe-Clin) and 3 wt.% Fe-ZSM-5 samples were synthesized by the ion-exchange procedure. The zeolite supports are clinoptilolite, a natural zeolite from Zeolado Company (Greece) and ZSM-5, a commercial zeolite from Alfa-Aesar (Si/Ai = 50:1). The ion-exchange synthesis procedure used to prepare the two catalysts is the following:

Briefly, clinoptilolite or ZSM-5 (1 g of powder) was addend into a backer with 250 ml of deionized water. Then, 0.217 g of iron(III) nitrate nonahydrate (Sigma-Aldrich, Germany) were added to the solution containing either clinoptilolite (Clin) or ZSM-5. The mixture was stirred for 2 h at 50°C and subsequently the slurry solution was centrifugated for 10 min. Then, the powder was washed with deionized water, dried overnight and finally calcinated at 550°C for 4 h.

2.2. Materials characterizations

The powder X-ray diffraction patterns were collected on an X'Pert Philips PW3040 diffractometer using Cu Kα radiation (2θ range = 5°–50°; step = 0.05° 2θ; time per step = 0.2 s). The diffraction peaks were indexed according to the Powder Data File database (PDF-2 1999, International Centre of Diffraction Data, PA, USA). The specific surface area (S_{BET}) and total pore volume (V_p) were measured by the N_2 physisorption at −196°C (Micromeritics Tristar II 3020, v1.03, Micromeritics Instrument Corp., Norcross, GA, USA, 2009) on samples previously outgassed at 200°C for 4 h. This step is necessary to eliminate adsorbed molecules on the zeolite surface (i.e. H_2O). The specific surface area of the samples was calculated using the Brunauer-Emmett-Teller (BET) method. The morphology of the samples was investigated by means of both a field emission scanning electron microscope (FESEM Zeiss MERLIN, Gemini-II column, Oberkochen, Germany) and a transmission electron microscope (the Tecnai G2 20, 200 KV). The Fe-content was determined by EDS analysis on several 10–50 nm diameter spots.

2.3. Catalytic activity

The AO7 conversion (%) was studied in dark condition by adding 1.0 g L^{-1} of catalyst powder (either Fe-Clin or Fe-ZSM-5) to 100 mL of 1.42 mM AO7 solution at natural pH of 6.80. The suspension was stirred at room temperature for 60 min.

To investigate the Fenton-type process, ascorbic acid (AA) and H_2O_2, along with the catalysts (Fe-Clin or Fe-ZSM-5) were considered for the AO7 degradation. The concentration of both AA and H_2O_2 in the AO7 solution was 2.67 10^{-3} M, in order to have the stochiometric balance with the Fe loaded.

Aliquots of the suspension were collected at regular intervals of time (namely at 10, 20, 30, 40, 50 and 60 min.), the supernatant fraction was separated by centrifugation (ALC centrifuge PK110, at 4,000 rpm for 2 min) and the UV–vis spectrum was measured in the 190–800 nm range on a Cary 5000 UV–vis–NIR spectrophotometer (Varian instruments), using a quartz cell with 1-mm path length. The concentration of AO7 was evaluated following the intensity at 484 nm, related to the hydrazone form (in equilibrium with the azo species, Fig. 1) by the UV-vis spectroscopy.

Degradation (%) of AO7 was calculated as $100\cdot(C_0–C_f)/C_0$ where C_0 and C_f are the initial and the final dye concentration (mM), respectively.

The initial rates (mmol s^{-1}) were calculated by the equation:

$$\text{Initial rate} = \frac{\text{AO7}_{\text{converted}}\,[\text{mmol/L}] \times 0.1\,[\text{L}]}{10\,[\text{min}] \times 60\,[\text{sec/min}]} \quad (1)$$

where the initial rate is considered in terms of mmol AO7 converted in a volume of 100 ml over a reaction time of 10 min.

3. Results and discussion

3.1. Physico-chemical properties

In Fig. 2 is reported the XRD patterns for all the samples.

Clin sample shows a high crystallinity, with intense peaks at 2θ = 9.92°, 22.43° and 30.50°, characteristic of the clinoptilolite material (reference code of the clinoptilolite: 00-039-1383) [13]. The peak at 2θ = 22.43° is the most intense peak of the clinoptilolite.

In the Fe-Clin sample, it is possible to observe: (i) a decrease of intensity; (ii) most of the diffraction peaks show the same position of the unexchanged sample; (iii) a small 2θ shift of the most intense peak results for the Fe-Clin (22.46°) as compared with the Clin (22.36°) (Fig. 2(b)).,. This finding suggests small changes in zeolite unite cell, with a possible shrinkage of the Clin framework due to the ion-exchange treatment with Fe^{3+} cations (ionic radius = 0.92 Å) able to remove larger cations i.e. K^+ (ionic radius = 1.18 Å) from the framework. The XRD patterns for the comparative samples (Fe-ZSM-5 and pure ZSM-5) exhibit the characteristic peaks of the ZSM-5 material, thus confirming the good stability of the material.

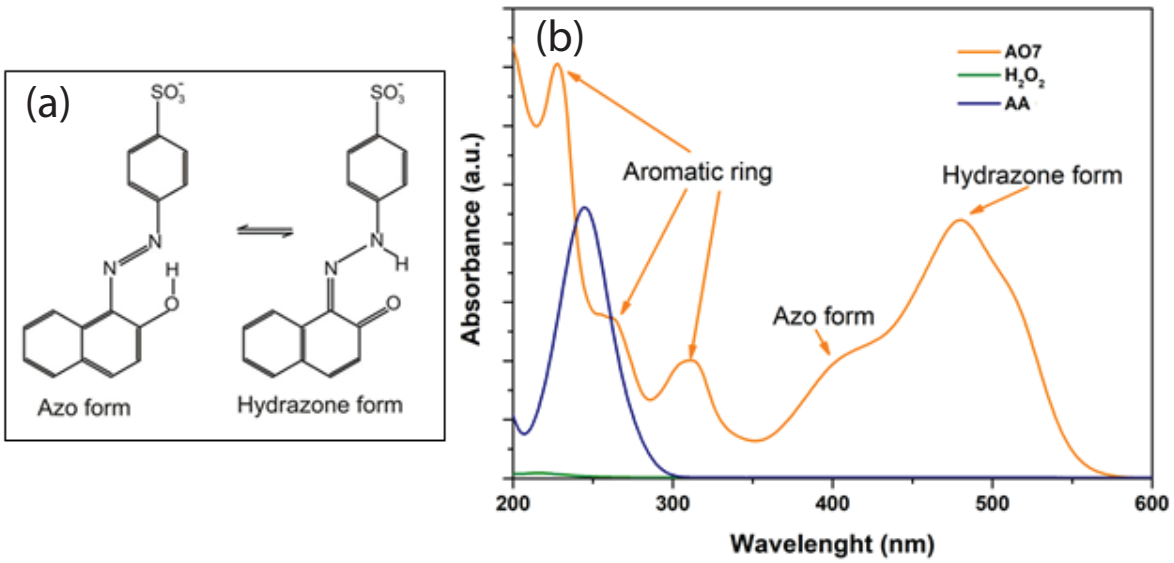

Fig. 1. Schematization of azo- and hydrazone structures of AO7 (1.42 mM) (a) along with the UV-Vis spectra of AO7 solution (1.42 mM), H_2O_2 (2.67 mM) and AA (2.67 mM) (b).

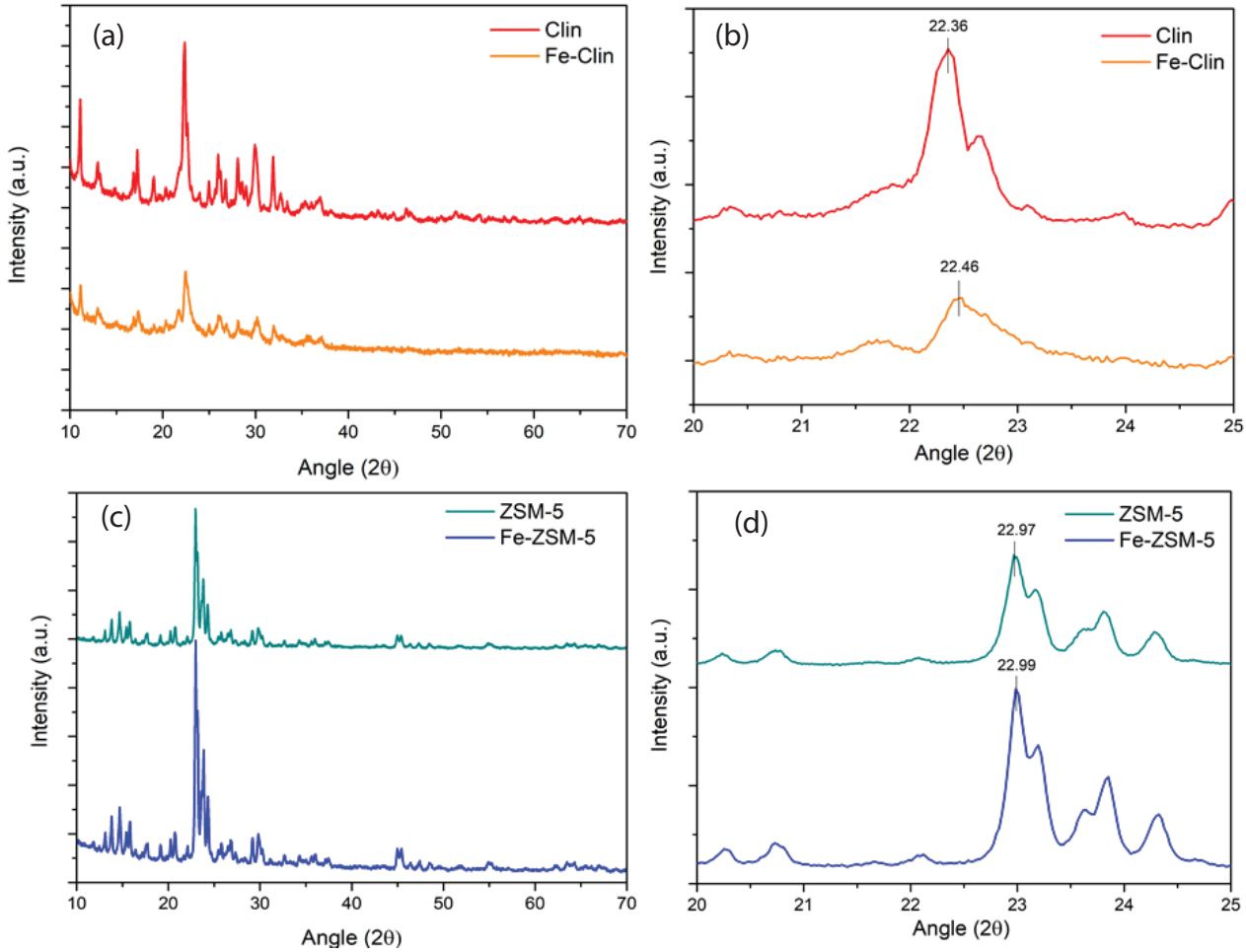

Fig. 2. XRD patterns of Clin and Fe-Clin (a) and their magnification (b). ZSM-5 and Fe-ZSM-5 (c) and their magnification (d).

Table 1 summarizes the specific surfaces areas (SSA) for the materials as derived by the N_2 physisorption at –196°C.

As expected, a lower (about one-tenth) SSA values can be observed for both the Clin and Fe-Clin samples as compared with the ZSM-5-type materials. The presence of Fe species into the framework does not modify the SSA of the clinoptilolite, whereas a significant reduction of the surface area can be observed for the Fe-ZSM-5, that may be due to the formation of several extra-framework FeO_x clusters on the MFI surface [14–16].

In Fig. 3 are shown the N_2 sorption isotherms for the samples previously outgassed at 200°C for 4 h.

Both the Fe-Clin and Clin samples exhibit similar isotherms and the capillarity condensation is followed by the H3-hysteresis, as observed elsewhere [17,18]. As is known, H3-hysteresis does not exhibit any limiting adsorption at high p/p^0. They are produced by aggregates of plate-like particles or assemblages of slit shaped pores and should not be expected to provide a reliable assessment of either the pore-size distribution or the total pore volume.

On the other hand, the presence of Fe species modifies the SSA for the ZMS-5-type material. The reason could be explained by the presence of Fe_xO_y clusters on the external surface of ZSM-5. These extra framework clusters could affect the average pore dimensions because occlude the ZSM-5 cavities. However, they did not modify the ZSM-5 structure, as confirmed by the XRD analysis (no-significant shift was observed between the XRD peaks of the Fe-ZSM-5 and those of the ZSM-5).

Table 1
Speficic surface areas (SSA) for the Clin, Fe-Clin, ZSM-5 and Fe-ZSM-5

Catalyst	SSA[a] (m^2g^{-1})
Clinoptilolite	36
Fe-Clinoptilolite	35
ZSM-5	412
Fe-ZSM-5	367

[a]Values calculated by the BET method.

Fig. 4 shows the FESEM images of the samples at comparable magnification. As expected, the clinoptilolite exhibits the flake-like structure where the particles are flat and stacked in layers [19].

When the Fe was incorporated in the clinoptilolite structure, the flakes look smaller and less compacted with the presence of smaller particles. This finding has been confirmed by the TEM analysis (Fig. 5): the Clin particles are bigger (up to few hundred nanometers) than those of the Fe-Clin sample. The clinoptilolite exhibits the characteristic flake-like shapes with average dimension of 35 nm of thickness and 120 nm of length. These information were found using ImageJ software by the analysis of FESEM and TEM images. Conversely, the ZSM-5 particles have an average diameter of 270 nm.

On the other hand, it is not possible to appreciate significant morphological differences between the Fe-ZSM5 and ZSM-5 samples.

The Fe-content (wt.%) in the zeolites was estimated by the EDS analysis on several areas (average values for the elements are reported in Table 2).

It appears that the Fe content in the Fe-Clin sample is 3.6 wt.%, whereas the amount of several other metals like K, Ca and Na, that decreased, thus suggesting an ion-exchange procedure for this sample. On the other hand, the typical composition of the clinoptilolite [9,20] was confirmed for the Clin sample. The comparative Fe-ZSM-5 sample exhibits a lower amount of Fe (2.1 wt.%).

3.2. Catalytic tests

The structural formula of the AO7 and its UV-Vis spectrum are shown in Fig. 1: the hydrazone form, stable in the solid phase, in aqueous solution under-goes an azo-hydrazone tautomerism, by an intra-molecular proton transfer [10–12]. The two peaks at 310 and 230 nm and the shoulder at 256 nm are due to aromatic rings absorptions whereas the peak at 484 nm is due to the n-π* transition involving the lone pair on N atoms and the conjugated system extending over the two aromatic moieties and encompassing the N–N group of the hydrazone form. The signal at 403 nm has a similar nature, involving the N–N group of

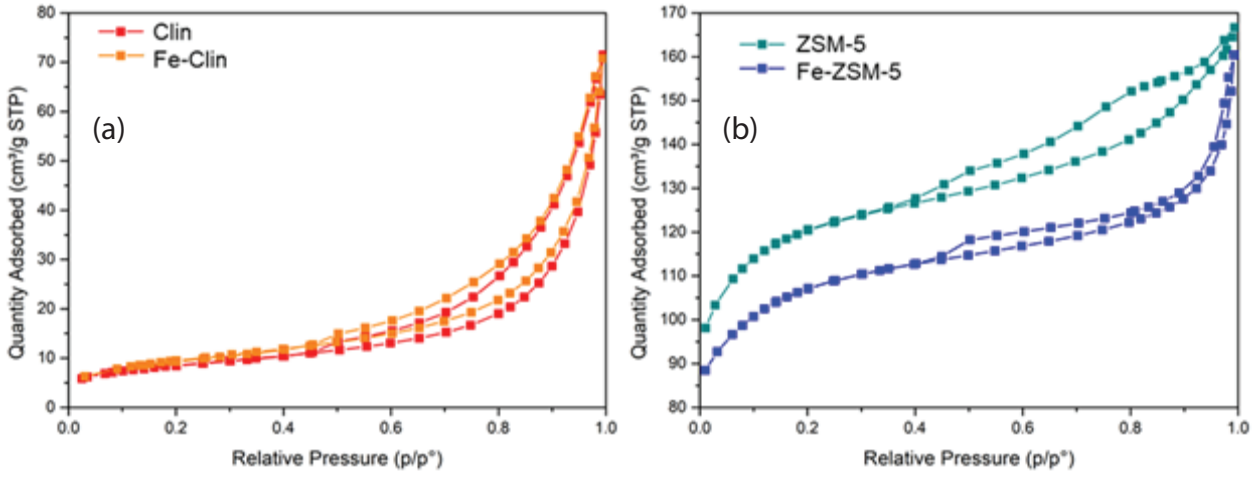

Fig. 3. N_2 adsorption/desorption isotherms at –196 °C for: Clin and Fe-Clin sample (a); ZSM-5 and Fe-ZSM-5 (b).

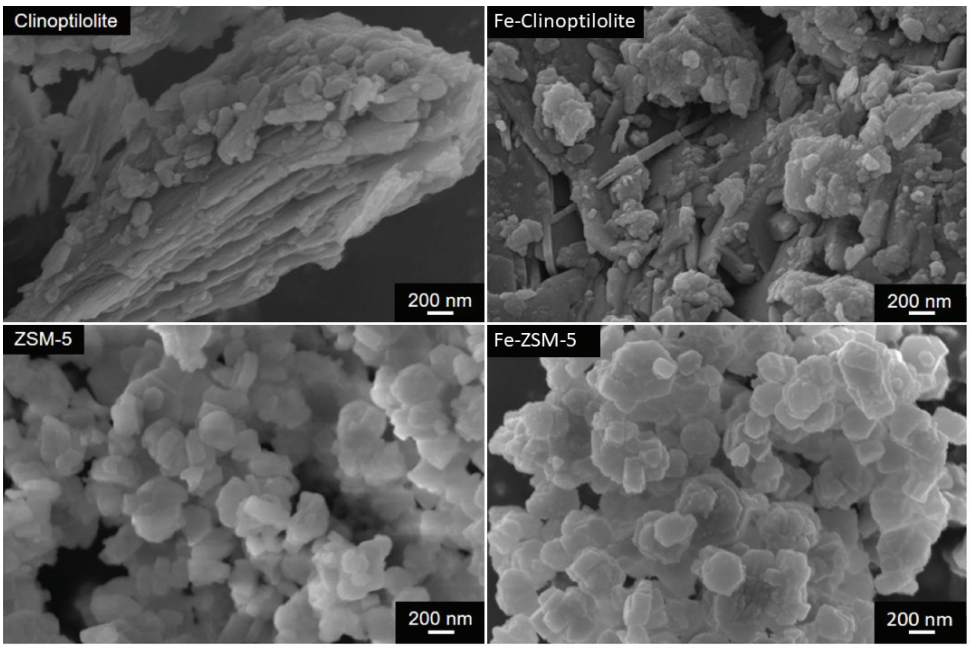

Fig. 4. FESEM images of the samples.

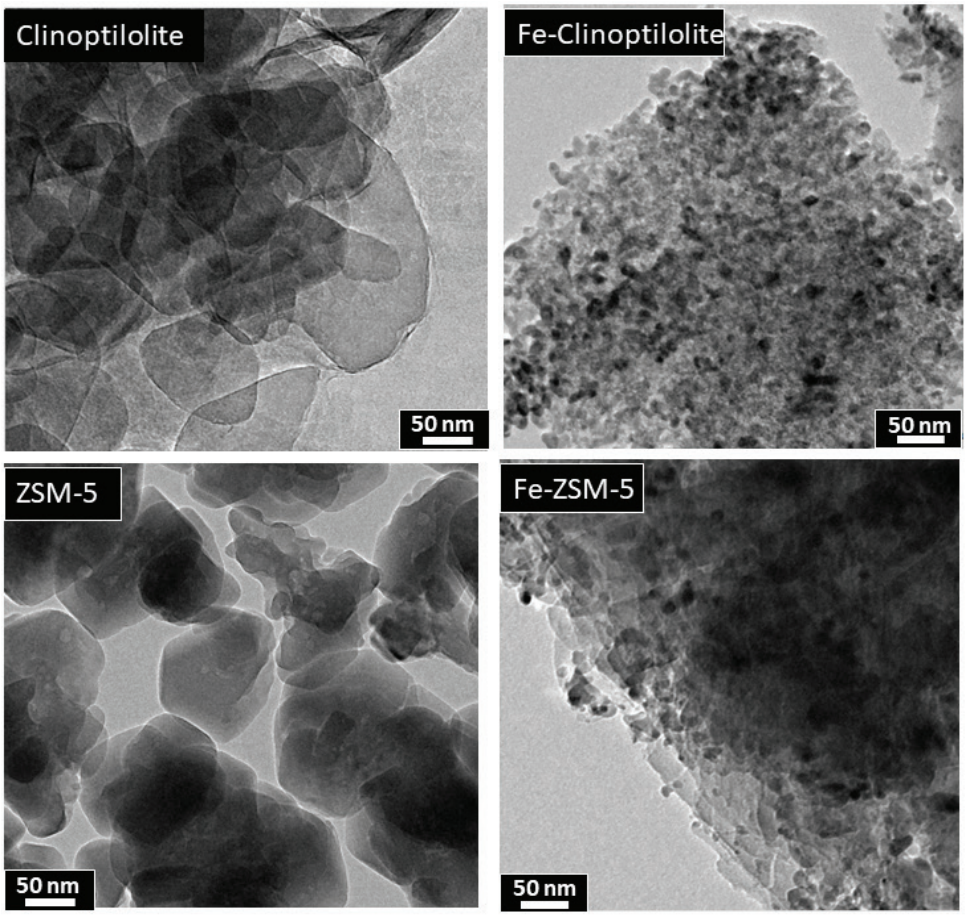

Fig. 5. TEM images of the samples.

the azo form. Absorbance spectra for AA and H_2O_2 are also reported for comparison purposes.

Fig. 6 compares the AO7 degradation in the absence of the catalysts. The (non-catalytic) reaction between AO7 and H_2O_2 was also studied. The UV–vis spectra taken with H_2O_2 are reported in Fig. 6(a): no change is observed in the AO7 bands over a reaction time of 60 min. Similar results were obtained for the reaction between AO7 and AA, as shown in Fig. 6(b). On the other hand, it appears that AO7 and H_2O_2/AA can react together to a small extent, as confirmed by a decrease in the band at 484 nm, reflecting of the AO7 degradation (Fig. 6(c)) [10–12,22,23]. In fact, about 30% of AO7 conversion is observed over a reaction time of 60 min.

Table 2
EDS values for the Clin, Fe-Clin and Fe-ZSM-5 samples

Element	Clinoptilolite weight (%)[a]	Fe-Clinoptilolite weight (%)[a]	Fe-ZSM-5 weight (%)[a]
O	41.7 ± 0.4	52.4 ± 0.4	55.2 ± 0.4
Si	39.9 ± 0.3	33.2 ± 0.33	40.7 ± 0.3
Al	7.8 ± 0.2	6.2 ± 0.15	1.5 ± 0.1
K	5.5 ± 0.2	2.2 ± 0.12	–
Ca	2.8 ± 0.2	2.0 ± 0.13	–
Fe	1.7 ± 0.2	3.6 ± 0.26	2.1 ± 0.2
Mg	0.5 ± 0.1	0.3 ± 0.06	–
Na	0.1 ± 0.00	–	–
N	–	–	0.5 ± 0.1
Total	100.00	100.00	100.00

[a]Values reported with their deviation standard.

Fig. 7 reports the UV–vis spectra of the AO7 solutions with the Fe-Clin sample, at different reaction times.

The only presence of the Fe-Clin catalyst in the AO7 solution does not activate any degradation process, as confirmed by the UV-spectra (Fig. 7(a)). The same results were observed for the degradation of AO7 with Fe-Clin and H_2O_2 (Fig. 7(b)).

The reaction between AO7 and Fe-Clin/AA produces few changes after 10 min, where the band at 484 nm decreases (degradation ~ 10%) and a band ca 250 nm increases (Fig. 7(c)). However, at longer times, it appears that reversible phenomena occur, suggesting adsorption/desorption processes rather than a real degradation of the AO7 molecule [22–23].

Noteworthy, an actual AO7 degradation occurs when the Fe-Clin is in presence of both AA and H_2O_2 (Fig. 7(d)). After only 10 min, the main band of AO7 decreases about 60% and then it stabilizes. This behavior could be ascribable to the consumption of the AA which is able to reduce the Fe^{3+} into Fe^{2+}: in this case, compare with Fig. 7(c), ferrous ions can react with AO7 molecules through radicals produced by H_2O_2.

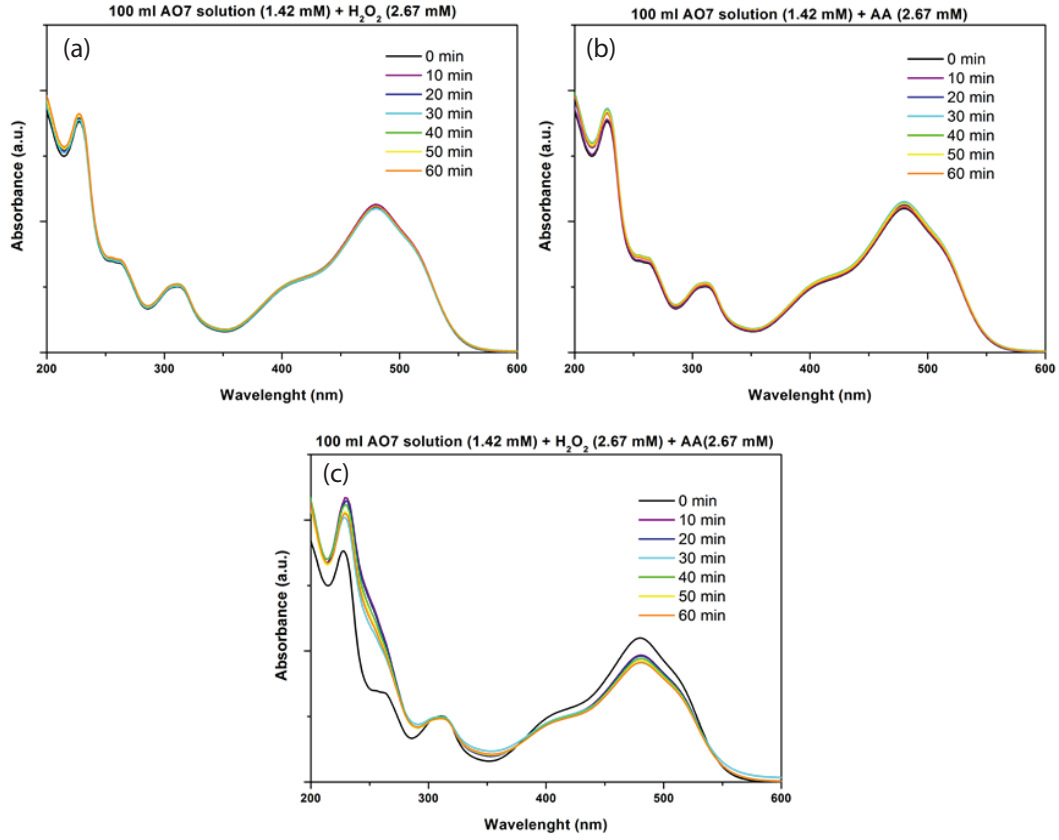

Fig. 6. UV-Vis spectra of AO7 solutions. Results obtained during the degradation of AO7 in the presence of H_2O_2 (a), AA (b) and AA/H_2O_2 (c). AO7 = 1.42 mM; pH 6.80; H_2O_2 = 2.67 mM; AA = 2.67 mM; AA/H_2O_2 (1:1) = 2.67 mM.

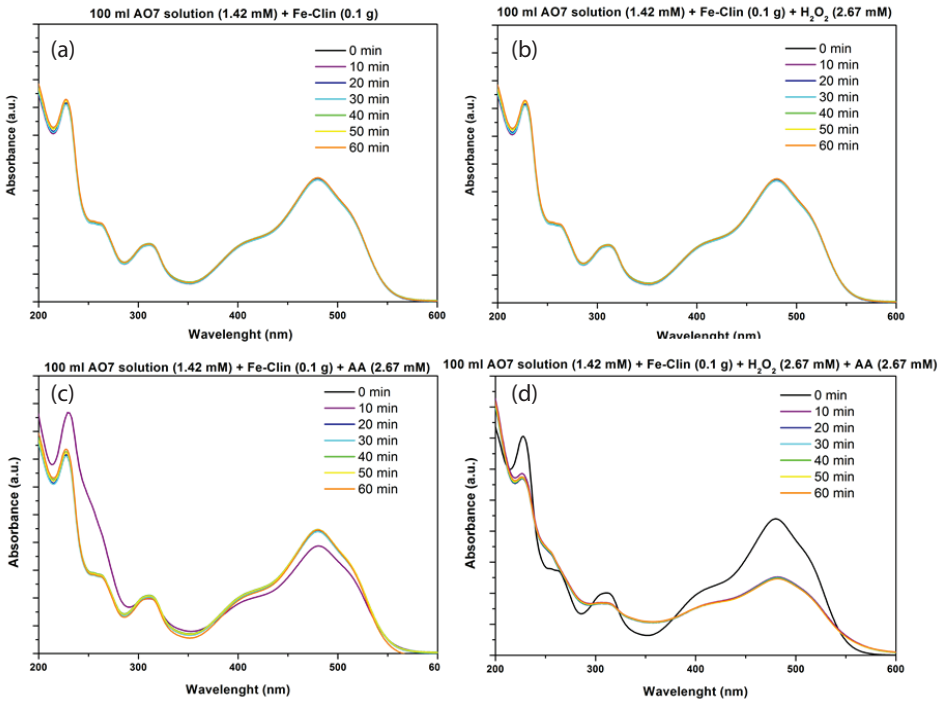

Fig. 7. UV-Vis spectra of different AO7 solutions. Results obtained during the degradation of AO7 in the presence of Fe-Clin (a), Fe-Clin/H_2O_2 (b), Fe-Clin/AA (c) and Fe-Clin/H_2O_2/AA (d). AO7 = 1.42 mM; pH 6.80; H_2O_2 = 2.67 mM; AA = 2.67 mM; AA/H_2O_2 (1:1) = 2.67 mM.

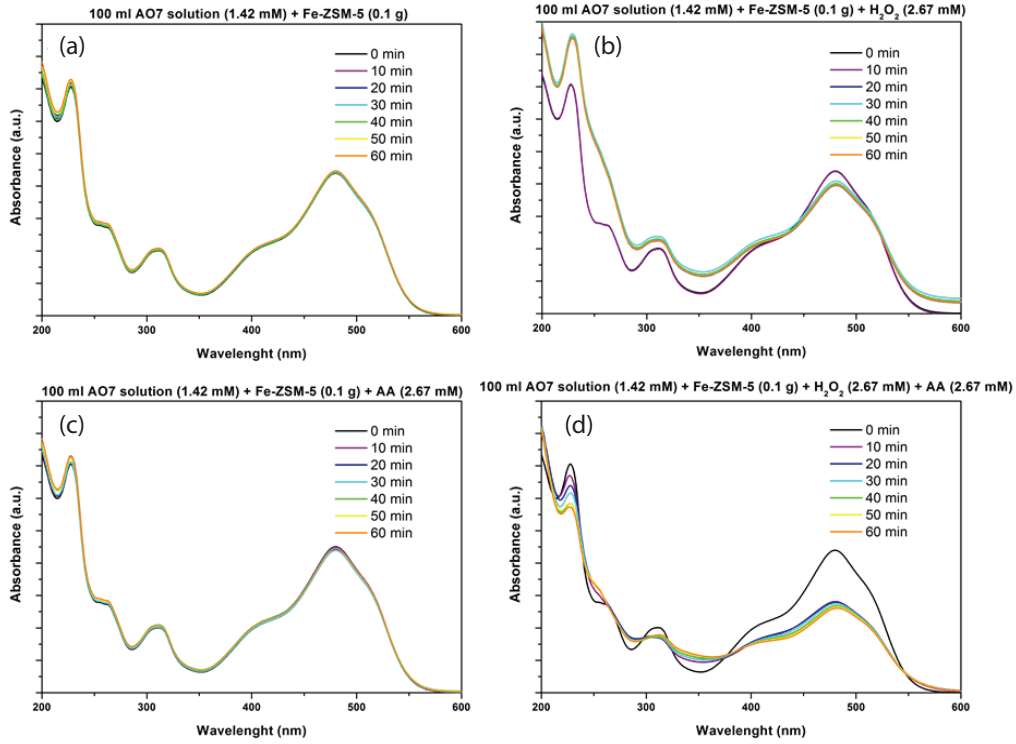

Fig. 8. UV-Vis spectra of different AO7 solutions. Results obtained during the degradation of AO7 in the presence of Fe-ZSM-5 (a), Fe-ZSM-5/H_2O_2 (b), Fe-ZSM-5/AA (c) and Fe-ZSM-5/H_2O_2/AA (d). AO7 = 1.42 mM; pH = 6.80; H_2O_2 = 2.67 mM; AA = 2.67 mM; AA/H_2O_2 (1:1) = 2.67 mM.

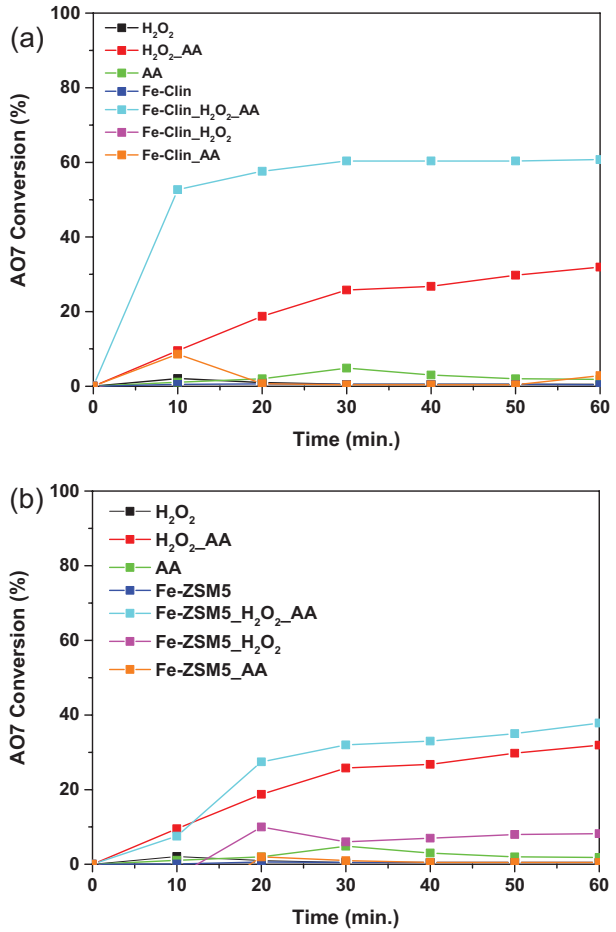

Fig. 9. Degradation of AO7 (conversion values, %) with Fe-Clin (a) and Fe-ZSM-5 (b) as a function of reaction time at different reaction conditions. AO7 = 1.42 mM; pH = 6.80; H_2O_2 = 2.67 mM; AA = 2.67 mM; AA/H_2O_2 (1:1) = 2.67 mM.

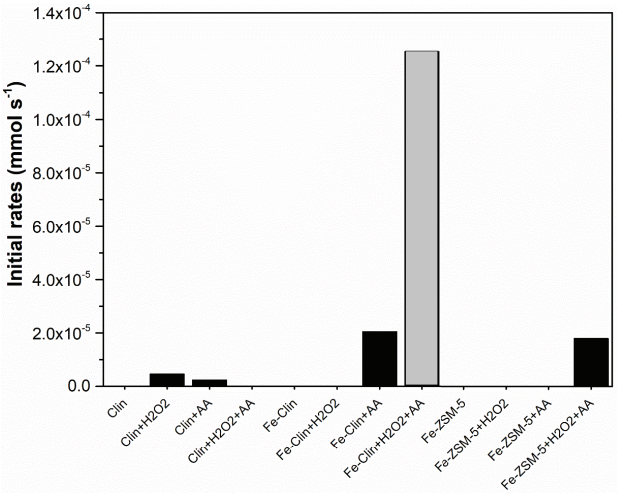

Fig. 10. Initial rates (mmol s^{-1}) for the degradation of AO7 with Fe-Clin, Clin, Fe-ZSM-5 and ZSM-5 samples at different reaction conditions. AO7 = 1.42 mM; pH = 6.80; H_2O_2 = 2.67 mM; AA = 2.67 mM; AA/H_2O_2 (1:1) = 2.67 mM.

Similar considerations can be extended to the degradation of the AO7 with the Fe-ZSM-5 catalysts (Fig. 8), thus confirming the results. In the present case, however, the AO7 degradation with the Fe-ZSM-5 in presence both AA and H_2O_2 appears worse compared with the Fe-Clin even if the much higher SSA of the commercial zeolite. A possible explanation of this result is the fact that different amounts (wt.%) of Fe are present into the two catalysts.

Fig. 9 summarizes the AO7 conversions (%) obtained with Fe-Clin (Fig. 9(a)) and Fe-ZSM-5 (Fig. 9(b)) as a function of reaction time at different reaction conditions. Results for non-catalytic reactions (namely, between AO7 and H_2O_2, AA, AA/H_2O_2) are also reported. As a whole, it is possible to observe that best performance (AO7 conversion ~ 60%) is achieved with the Fe-Clin in presence both AA and H_2O_2. This result confirms the important role of both oxidant and reductant agents in Fenton-like processes.

In fact, the presence of Fe species and H_2O_2 leads to a Fenton-type process effective for the AO7 degradation, as follows:

$$Fe^{2+} + H_2O_2 \rightarrow Fe^{3+} + OH^- + HO\cdot \quad (2)$$

$$Fe^{3+} + H_2O_2 \rightarrow Fe^{2+} + H^+ + HO_2 \quad (3)$$

$$HO\cdot + H_2O_2 \rightarrow HO_2\cdot + H_2O \quad (4)$$

$$HO_2\cdot + H_2O_2 \rightarrow HO\cdot + H_2O + O_2 \quad (5)$$

$$AO7 + HO \rightarrow \text{degradation products} \quad (6)$$

Both the Fe^{2+} and Fe^{3+} species seem to be active for Fenton-type processes, although Fe^{3+} leads to slower kinetics [12,22–24]. However, our recent studies [10–12,21] confirmed the beneficial role of the co-presence of H_2O_2 and AA to promote the Fenton-like processes in the presence of transition metals with high oxidation state (namely V and Fe). AA and H_2O_2 lead to the formation of higher amounts of radicals, the key products in the Fenton chemistry. As a result, the presence of both oxidant and reductant enhance the overall reactivity of the Fenton-like process.

In order to compare the results for the AO7 degradation using different catalytic systems, the initial rates are reported in Fig. 10. The latter confirms the highest initial rate for the Fe-Clin_H_2O_2_AA system (1.25 10^{-4} mmol s^{-1}), followed by the Fe-Clin _AA (2.05 10^{-5} mmol s^{-1}) and then Fe-ZSM-5_H_2O_2_AA (1.79 10^{-5} mmol s^{-1}).

4. Conclusions

In this study we demonstrated that a natural zeolite (clinoptilolite) can undergo to an easy cation-exchange to increase the amount of naturally iron present and therefore it can be more efficiently used in wastewater remediation. We prepared a 3 wt.% Fe-Clin sample which shows good performances for the AO7 degradation in presence of both H_2O_2 and AA. Similarly, a Fe-containing ZSM-5 material was prepared for comparison. Both samples, along with the unexchanged zeolites were characterized by complementary techniques. Wastewater remediation

tests were performed with AO7 solutions to investigate the Fenton-type activity in the presence of AA and H_2O_2. Interestingly, the best performances (in terms of initial rates and AO7 conversion values) were observed for the Fe-Clin sample. This finding suggests that Fe-containing natural zeolites can be used for Fenton-type processes in wastewater remediation.

Acknowledgements

Support of Zeolado in providing the clinoptilolite used through the investigation is gratefully acknowledged.

TEM analysis was done thanks to the project RheoCom ''Rheology of complex materials containing nano-sized components for civil engineering applications'' funded by Politecnico di Torino and Compagnia di SanPaolo, Turin, Italy.

F.S. Freyria thanks CARIPLO foundation, grant number 2015–0186 DeN–Innovative technologies for the abatement of N-containing pollutants in water.

References

[1] L. Pauling, The structure of some sodium and calcium aluminosilicates, Proc. Natl. Acad. Sci. USA, 16 (1930) 453–459.
[2] W.H. Taylor, I. The structure of analcite ($NaAlSi_2O_6$ H_2O), Z. Krist. - Cryst. Mater., 74 (1930) 1–19.
[3] L. Pauling, Kristallgeometric Kristallphys, Z. Krist., 74 (1930).
[4] M. Sprynskyy, B. Buszewski, A.P. Terzyk, J. Namieśnik, Study of the selection mechanism of heavy metal (Pb^{2+}, Cu^{2+}, Ni^{2+}, and Cd^{2+}) adsorption on clinoptilolite, J. Colloid Interface Sci., 304 (2006) 21–28.
[5] G. Blanchard, M. Maunaye, G. Martin, Removal of heavy metals from waters by means of natural zeolites, Water Res., 18 (1984) 1501–1507.
[6] M.D. Lewis, Clinoptilolite, as a N, K, and Zn source for plants, 1981.
[7] T.S. Perrin, D.T. Drost, J.L. Boettinger, J.M. Norton, Ammonium-loaded clinoptilolite: a slow-release nitrogen fertilizer for sweet corn, J. Plant Nutr., 21 (1998) 515–530.
[8] F.S. Freyria, M Armandi, M Compagnoni, G Ramis, I Rossetti, B Bonelli, Catalytic and photocatalytic processes for the abatement of N-containing pollutants from wastewater. Part 2: organic pollutants, J. Nanosci. Nanotechnol., 17 (2017) 3654–3672.
[9] M. Dosa, M. Piumetti, S. Bensaid, N. Russo, O. Baglieri, F. Miglietta, D. Fino, Properties of the clinoptilolite: characterization and adsorption tests with methylene blue, J. Adv. Catal. Sci. Technol., 5 (2018) 1–10.
[10] M. Piumetti, F. Freyria, M. Armandi, F. Geobaldo, E. Garrone, B. Bonelli, Degradation of Acid Orange 7 by transition metals containing mesoporous titania in the presence of H_2O_2 and ascorbic acid, Catal. Struct. React., 33 (2013) 10–11.
[11] M. Piumetti, F.S. Freyria, M. Armandi, G. Saracco, E. Garrone, G.E. Gonzalez, B. Bonelli, Catalytic degradation of Acid Orange 7 by H_2O_2 as promoted by either bare or V-loaded titania under UV light, in dark conditions, and after incubating the catalysts in ascorbic acid, Catal. Struct. React., 1 (2015) 183–191.
[12] F. Freyria, M. Compagnoni, N. Ditaranto, I. Rossetti, M. Piumetti, G. Ramis, B. Bonelli, Pure and Fe-doped mesoporous titania catalyse the oxidation of acid orange 7 by H_2O_2 under different illumination conditions: Fe doping improves photocatalytic activity under simulated solar light, Catalysts, 7 (2017) 213.
[13] A. Arcoya, J.A. Gonzalez, N. Travieso, X.L. Seoane, Physicochemical and catalytic properties of a modified natural clinoptilolite, Clay Miner., 29 (1994) 123–131.
[14] M. Piumetti, B. Bonelli, P. Massiani, S. Dzwigaj, I. Rossetti, S. Casale, L. Gaberova, M. Armandi, E. Garrone, Effect of vanadium dispersion and support properties on the catalytic activity of V-SBA-15 and V-MCF mesoporous materials prepared by direct synthesis, Catal. Today, 176 (2011) 458–464.
[15] M. Piumetti, B. Bonelli, P. Massiani, Y. Millot, S. Dzwigaj, L. Gaberova, M. Armandi, E. Garrone, Novel vanadium-containing mesocellular foams (V-MCF) obtained by direct synthesis, Microporous Mesoporous Mater., 142 (2011) 45–54.
[16] P. Castaldi, L. Santona, S. Enzo, P. Melis, Sorption processes and XRD analysis of a natural zeolite exchanged with Pb^{2+}, Cd^{2+} and Zn^{2+} cations, J. Hazard Mater., 156 (2008) 428–434.
[17] M. Piumetti, N. Russo, Notes on catalysis for environment and energy, Torino, 2017.
[18] K.S.W. Sing, Reporting physisorption data for gas/solid systems with special reference to the determination of surface area and porosity, Pure Appl. Chem., 57 (1985) 603–619.
[19] F.A. Mumpton, W.C. Ormsby, Morphology of zeolites in sedimentary rocks by scanning electron microscopy, Clays Clay Miner., 24 (1976) 1–23.
[20] G. Tsitsishvili, T. Andronikashvili, G. Kirov, L. Filizova, Natural Zeolites, Chichester, 1991.
[21] M. Piumetti, F.S. Freyria, M. Armandi, F. Geobaldo, E. Garrone, B. Bonelli, Fe- and V-doped mesoporous titania prepared by direct synthesis: characterization and role in the oxidation of AO7 by H_2O_2 in the dark, Catal. Today, 227 (2014) 71–79.
[22] F.S. Freyria, B. Bonelli, R. Sethi, M. Armandi, E. Belluso, E. Garrone, Reactions of acid orange 7 with iron nanoparticles in aqueous solutions, J. Phys. Chem. C, 115 (2011) 24143–24152.
[23] F.S. Freyria, S. Esposito, M. Armandi, F. Deorsola, E. Garrone, B. Bonelli, Role of pH in the aqueous phase reactivity of zerovalent iron nanoparticles with Acid Orange 7, a model molecule of azo dyes, J. Nanomater., 2017 (2017) 1–13.
[24] M. Piumetti, F.S. Freyria, B. Bonelli, Catalytically active sites and their complexity: a micro-review, Chem. Today, 45 (2013) 55–58.